Cement & Concrete Composites 32 (2010) 580–588

Contents lists available at ScienceDirect

Cement & Concrete Composites

journal homepage: www.elsevier.com/locate/cemconcomp

Mechanical behaviour of Textile Concrete under accelerated ageing conditions

S.W. Mumenya [a,*], R.B. Tait [b], M.G. Alexander [c]

[a] Department of Civil and Construction Engineering, University of Nairobi, Kenya
[b] Department of Mechanical Engineering, University of Cape Town, South Africa
[c] Department of Civil Engineering, University of Cape Town, South Africa

ARTICLE INFO

Article history:
Received 5 April 2008
Received in revised form 5 July 2010
Accepted 11 July 2010
Available online 14 July 2010

Keywords:
Cementitious materials
Mechanical behaviour
Mechanical properties
Fibre pull-out
Fibre/matrix interface
Bonding
Environmental exposure
Textile Concrete

ABSTRACT

The mechanisms of ageing and environmental degradation involving exposure to cyclic hot/cold temperatures, wetting/drying movements as well as exposure to a carbon dioxide (CO_2)-rich environment, have different effects on the microstructure of interfaces within cementitious composites. This paper presents results of an investigation into changes occurring in fibre pull-out and composite tensile behaviour in Textile Concrete (TC) after exposure to accelerated ageing conditions. The microstructure of the matrix at the fibre/matrix interface, and fibre properties, were found directly to affect the mechanical behaviour at the macro-level. The study illustrated that exposure of TC to a CO_2-rich environment improves the fibre/matrix bond significantly; no major changes were observed in the mechanical behaviour of the composites after exposure to hot/cold and wetting/drying environments.

1. Introduction

The service life of a material is to a great extent dependent on environmental exposure conditions, duration of exposure (time), and properties of its constituents. This is equally true of Fibre Reinforced Cementitious Composites (FRCC), which are finding increasing use as construction materials today. These materials are essentially three phase materials comprising a matrix or binder phase, a reinforcing or fibre phase, and a fibre/matrix interface phase. This latter phase is of great importance in FRCC since its properties have a profound influence on the properties of the composite material. It is also often the phase in which long-term effects create the greatest change in mechanical properties mainly due to changes in fibre/matrix bonding characteristics. The microstructure of FRCC has been shown to vary with the processing technique, matrix composition, fibre surface properties, curing conditions, and age [1,2].

In modern building technology, conventional materials are used in new ways and new materials are used without long-term experience. It is important that the behaviour of a material in service be predictable, which is commonly based on prior experience with materials in similar applications. In the absence of past experience, prediction is based on accelerated ageing tests, which create a better understanding of the mechanisms that bring about physical changes at the microstructure level.

The physical changes at the fibre/matrix interface are often environmentally-related mainly due to changes in the matrix microstructure. Cement paste (or mortar) continues to change as hydration reaction progresses, which usually leads to an increase in strength and stiffness. The rate of hydration varies with temperature and moisture state; therefore cyclic hot/cold, wet/dry environments are possible mechanisms of microstructural change. Variations in the moisture state affect the specific surface area and pore size distribution whereas temperature accelerates the hydration reaction [1].

Microstructural changes in cementitious materials are due to physical or chemical factors which are often associated with environmental exposure. The mechanisms of physical attack are abrasion, erosion such as in wetting/drying environments, cavitation, or expansive reaction such as freeze–thaw. On the other hand, chemical attack is driven by dissolved gases and liquids, which cause sulphate attack, alkali-silica reaction, and carbonation [3]. The rate of ingress of fluids into concrete increases with temperature and humidity [4]. Cyclic action of temperature and moisture that is common in some tropical environments has been attributed to leaching of concrete and subsequent propagation of microcracks [5]. The physical effects of thermal changes are volume movements which induce stresses in the microstructure leading to increase in microcracking in concrete. Gases and fluids are absorbed and

* Corresponding author. Tel.: +254 722 705191; fax: +254 2 3875323.
E-mail addresses: wsiphila@uonbi.ac.ke, msiphila@ymail.com (S.W. Mumenya).

0958-9465/$ - see front matter Crown Copyright © 2010 Published by Elsevier Ltd. All rights reserved.
doi:10.1016/j.cemconcomp.2010.07.007

retained within the microcracks where they cause physical and chemical expansive reactions.

Air contains carbon dioxide (CO_2) which, in the presence of moisture, causes a carbonation reaction to proceed in cementitious materials resulting in deposition of calcium carbonate ($CaCO_3$) in the microstructure. This occupies a greater volume than replaced calcium hydroxide ($Ca(OH)_2$), leading to reduction in the porosity of carbonated concrete [2]. In addition, water released by $Ca(OH)_2$ on carbonation may aid in the hydration of cement. These changes are beneficial in that they result in increased strength, and reduced permeability and moisture movement. However, carbonation induces volume changes that cause shrinkage which may induce cracking [2]. In reinforced concrete, carbonation environment exposes the steel to corrosion leading to premature deterioration.

All these effects, which occur during long-term ageing of FRCC, have important influence on the durability and serviceability of the material. At the fibre/matrix interface, chemical and physical changes occur after exposure to different environments, which affect the nature of bonding.

Textile Concrete (TC) is produced from cement paste or mortar, reinforced with textiles which are formulated for use in cementitious matrices. Where polymeric textiles are used, polypropylene (PP) is commonly chosen due to its low cost and a combination of very attractive properties, namely resistance to chemical attack in the highly alkaline cement medium, resistance to degradation under moist environments, high elongation at break with low specific gravity, and no major handling difficulties.

There is growing interest in mechanical characterisation of TC but being a relatively new product, TC technology is still at its infancy with sparse information, particularly on its mechanical performance under different environments. Thus the durability or long-term performance of TC is still a major concern and there is need for assessment of the long-term mechanical behaviour. This research is primarily an experimental study based on accelerated ageing under different exposure conditions.

The study found that no significant change was observed in the fibre/matrix bond strength after either cyclic hot/cold or wet/dry environments, but there was a marked strength increase of approximately 18% after carbonation exposure. The effects of these changes on mechanical behaviour of TC are largely the focus of this paper.

Different types of fibres have been suggested as suitable reinforcement in FRCC such as: asbestos, steel, glass, carbon, natural fibres (such as cellulose and sisal), and various types of polymeric fibres such as polypropylene (PP) [6]. PP fibres have good chemical resistance, are relatively inert to moisture at normal ambient temperatures, have high elongation at break with low relative density, and are easily handled after appropriate processing [7]. With ongoing research on alternatives to asbestos fibres, it is believed that PP fibres have many advantages as a possible alternative to not only asbestos, but also glass, steel and cellulose. Development of PP fibres for cement reinforcement, where proprietary surface treatment is applied to enhance the wetting and the compatibility with the matrix, has accelerated growth in new industries such as Textile Concrete (TC). TC is essentially a fine grained cementitious matrix reinforced with layers of two dimensional mesh fabric. In South Africa, the textile is made of PP which is specially formulated for use in cementitious matrices.

Alkali Resistant (AR) glass fibres have been used in production of Glass Fibre Reinforced Concrete (GRRC), a composite which has been in the forefront in development of new applications of TC such as: integrated formwork and exterior cladding panels, decorative elements, ducts and channels, bridge parapets and many more [8]. Carbon fibres have been used together with polymeric fibres in production of concrete tubes, and a significant enhancement of the flexural strength of the composite is reported [9].

A recent study of the mechanical behaviour of Textile Concrete characterised pseudo-ductile behaviour under flexural and direct tensile loading [10]. However, the durability and long-term performance of this new material is still a major concern and there is need for the development of a reliable method for assessment of the long-term behaviour [11,12]. By accelerating the ageing of TC samples, an attempt was made to assess the long-term behaviour of TC, reported here. There are no clear guidelines or standard procedures for accelerated ageing of FRCC. In addition, since TC is still a new material, there is scarcity of data on its natural ageing or long-term performance [13–19]. Therefore, in this study, the accelerated ageing procedure was guided partly by past work on conventional FRCC reported in the literature [20], and partly by practical considerations. Three regimes were chosen based on tropical and moderate climates. The regimes were hot/cold, wet/dry, and 10% accelerated carbonation.

2. Materials and experimental details

2.1. Fibres

Fibrillated forms of PP fibres were chosen for this study because fibrillation improves mechanical bonding with cement matrices [6]. However, despite improving the mechanical properties of the fibres, the fibrillation process weakens the film in the lateral direction. To address this concern and improve interaction and mechanical bonding with the cementitious matrix, continuous PP fibres with an extended fibrous surface were chosen for this research. The fibres, referred to here as 'hybrid fibres', were specially produced in South Africa and designed for use with cement matrices.

The 'hybrid fibres' consist of fluffy layers of PP fibrils spun around two strands of fibrillated tapes of polymeric fibres as the core in order to provide a substantial mechanical bond with the cement matrix. The 'hybrid fibre' provides the basis for achieving sufficient strength and controlled bonding with cementitious matrix.

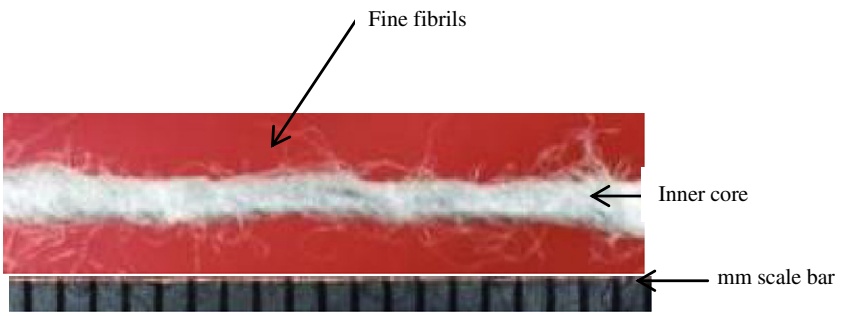

Fig. 1. Typical 'hybrid fibre'.

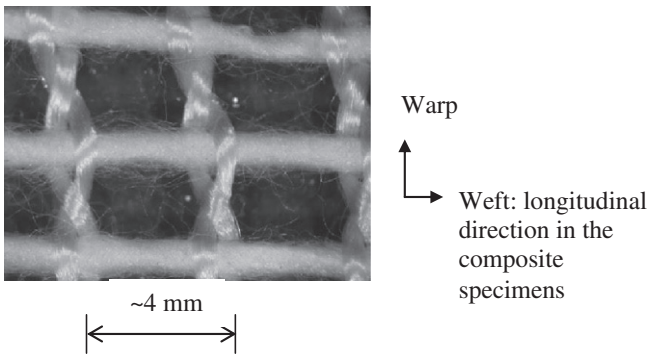

Fig. 2. The textile showing warp and weft directions.

This fibre is then woven into a matrix cloth to provide the desired properties. The woven textile is easily placed in the cement composite in the appropriate location and orientation, for optimum performance and with very high fibre volume fractions (in excess of 10%). The density of the PP fibres was 0.94 g/cm^3 and the cross-sectional area was 0.303 mm^2. The average tensile strength and stiffness of the fibres prior to environmental exposure were approximately 77 N and 1077 MPa, respectively. Fig. 1 shows a 'hybrid fibre' that was used for this study.

2.2. Textile

The textile used for production of TC composites was manufactured in conventional mills. The yarn in the weft direction was a 'hybrid fibre' illustrated in Fig. 1, whereas in the warp direction, two strands of fibrillated polypropylene fibres were used. The textile is woven into a mesh, commercially referred to as 'CemForce', illustrated in Fig. 2.

The inner tapes of the textile had a cross section of approximately 1.0 mm × 0.3 mm, aperture size of 4 mm × 4 mm, and the mass per unit area of 87 g/m^2. Tensile tests were performed on 100 mm × 50 mm samples of the textile using a universal testing machine, which was programmed for a ramp rate of 10 mm per minute and a maximum displacement of 100 mm. The average ultimate tensile strength of the textile in the warp and weft directions was 20 kN/m.

2.3. Cementitious mixture composition

The binder was a thoroughly blended mixture of ordinary Portland cement designated CEMI 42.5, and Ultra-Fine Fly Ash (UFFA) locally referred to as 'Superpozz', with 90% of particles finer than 11 μm. The mix needed to be such that compaction was easily achievable, together with good mechanical properties, while at the same time striving to be reasonably comparable with 'normal' practice. To achieve an appropriate mix, coarse aggregate was avoided and dune sand with maximum size 600 μm, fineness modulus of 1.71 and controlled moisture content (air dry) was employed. The density of the sand was 2.60 g/cm^3. A sand/binder ratio of 1.0 was used, with nominal water: binder ratio of 0.5. 'Superpozz' was used at a cement replacement level of 10% by mass, primarily to assist in achieving flow.

Mixing was undertaken for two minutes in a Hobart A120 planetary mixer, and the flow characteristics determined using the ASTM flow table test [21]. This entailed the mix being placed via a cone onto the flow table at a specified time after mixing, and its flow characteristics (diameter as a function of jolt impacts) being determined. The mortar mix had a minimum setting time of two hours and had minimum segregation and bleeding. The matrix was characterised by cube crushing strength of samples which were subjected to the same environmental regimes as the composites. Control samples were water-cured for 28 days at 23 °C; thereafter at 20 °C and Relative Humidity of 53% for different period ranging from 8 months to 20 months. The density and cube crushing strength of the samples at different ages and exposures are shown in Table 1.

2.4. Specimen production

The "hybrid fibre" shown in Fig. 1 was used for the single fibre pull-out test, and in the longitudinal direction (weft in Fig. 2) in the composite tests. In the present study, single fibre pull-out and composite tensile tests were performed. Specimens for fibre-pull-out tests were cast in specially made moulds to form symmetrical mortar briquettes of nominal thickness 8 mm and with the geometry shown in Fig. 3. To ensure that failure occurred by fibre pull-out other than rupture, trial tests were undertaken which indicated that an embedded fibre length (l_e) of 22 mm was suitable. The samples were cast by first filling the mould to mid depth and then locating the fibre longitudinally in the mould. The fibre was centrally held in position by threading it through two acetate sheets to separate the specimen; thereafter mortar was added to full mould depth, followed by gentle shaking to ensure sufficient impregnation of the fibre with mortar to facilitate satisfactory experimentation. The acetate sheets facilitated tensile strength evaluation of the fibre pull-out itself, without being masked by any tensile strength of the paste. After setting, the specimens were wet-cured at a temperature of 21 °C for 28 days followed by condi-

Table 1
Characteristics and mechanical properties of constituent materials.

Fibre sample				Mortar sample			
Exposure condition	Average peak load (N)	Modulus E_f (MPa) average	% failure strain	Exposure condition	Age at test	density (g/cm^3)	Cube strength (MPa)
Control (tested dry)	77.3	1077	26.7	Control	3 days	2.060	10.8
Control (tested wet)	80.4	878	30.2	Control	7 days	2.090	20.8
100 hot/cold cycles 23–50 °C	60.8	566	36.1	Control	28 days	2.060	35.2
100 wet/dry cycles at 35 °C	73.4	1123	22.4	Control	8 months	2.000	36.9
				Hot/cold		1.936	30.8
Carbonated at 30 °C and 55% RH	62.1	612	33.3	Control	10 months	2.080	44.4
				Wet/dry		2.136	64.8
12 months in a moderate climate	76.5	1678	16.5	Control	12 months	2.064	48.0
				Carbonated		2.072	64.4
				Moderate climate		2.147	56.8
12 months in a tropical climate	40.0	1292	9.6	Control	20 months	2.040	62.1
				Tropical climate		2.050	66.0

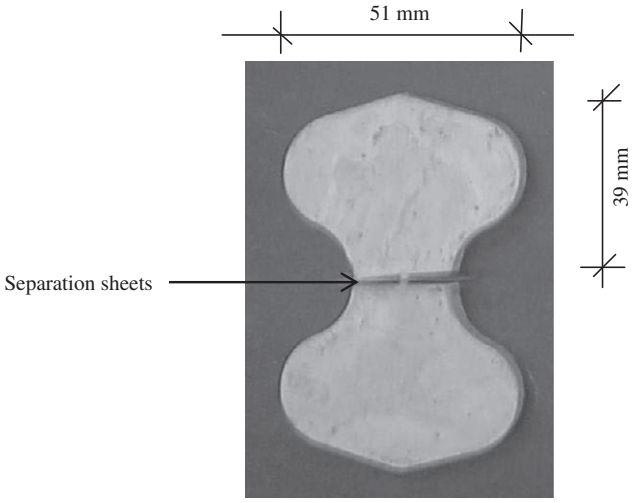

Fig. 3. Fibre pull-out specimen.

tioning at 55–60% relative humidity and 23 °C in an environmentally controlled room. Fifteen specimens were cast for each of the three exposure regimes: hot/cold, wet/dry, carbonation; and for control specimens.

The geometry of the composite TC tensile specimen and the gripping system were customised to be adaptable to the standard fixtures of a ZWICK Universal Testing Machine. The specimen had a gauge length of 125 mm, width over gauge length of 50 mm, and the overall length was 300 mm. The gripping area was smoothly rounded into the gauge sections with 100 mm radii. The widest section at the gripping area was therefore 90 mm, reducing to 50 mm over a length of 50 mm. Composite samples were produced using a hand lay-up technique whereby mortar was worked into six layers of CemForce to produce laminates with a nominal thickness of 8 mm, which was considered thin enough for gases and moisture to permeate during the tests. The specimen used for the tensile test is shown in Fig. 4. Ten specimens were cast for each of the exposure regimes and for controls.

2.5. Accelerated ageing

Ageing of TC samples was achieved by means of a dedicated accelerated ageing environmental facility. The facility consisting of two independent systems; hot/cold, and wet/dry, was operated in a semi-automated state. Heating was by three halogen light bulbs, and water cooling (but not wetting) simulated a cold environment. The temperature range in the hot/cold chamber was between 23 °C and 50 °C. A 75 min cycle time comprising 30 min heating and 45 min cooling periods was found suitable.

The accelerated ageing facility had a chamber adjacent to the hot/cold chamber which facilitated wetting and drying of specimens by drawing a vacuum of approximately-97 kPa to extract the moisture. To help evaporate water at a vacuum of −97 kPa, the temperature was elevated to approximately 35 °C. The temperature inside the wet/dry chamber was controlled by use of a heating element (with an in-built thermostat) that was positioned horizontally at mid-height of the chamber. Therefore the temperatures in the wet/dry chamber varied between 23 °C during wetting and 35 °C during the drying cycle. The wet/dry system was controlled by a timer relay with a wetting cycle time of 30 min and about 5 h drying period, which were based on drying trial tests. One hundred cycles were chosen both for hot/cold and wet/dry regimes.

Carbonation was facilitated through a chamber operating at a temperature of approximately 30 °C, and relative humidity (RH) between 55% and 70%. The CO_2 concentration was 10%, and the carbonation depths were monitored from time to time using phenolphthalein indicator [22]. Complete carbonation was observed after 6 months.

Control samples were wet-cured at a temperature of 21 °C for 28 days followed by conditioning at 55–60% relative humidity and a temperature of 23 °C in an environmentally controlled room. The control samples were tested at ages 5, 8, and 12 months. Samples which were conditioned for approximately 4 months were separated into three batches for weathering in hot/cold, wet/dry, and carbonation environments. The samples weathered in a hot/cold environment were tested at age 12 months, wet/dry-weathered samples were tested at age 14 months, and carbonated samples were tested at age 16 months.

2.6. Fibre pull-out tests

Fibre pull-out tests were conducted on a ZWICK UTM illustrated schematically in Fig. 5a. The tests were based on the ASTM tensile test method for cement paste [23], together with developments by Currie and Gardiner [24] and Tait and Guddye [25]. Each sample was centrally positioned within the grips of the testing machine, care being taken to avoid eccentricity in the loading. The samples were loaded in uni-axial tension under displacement control, at a rate of 10 mm/min. The specimens were loaded to failure, which was characterised by complete pull-out of one side of the PP fibre. Load was measured by a 10 kN capacity load cell with an accuracy of 0.5%. Displacement was measured directly from the crosshead of the UTM, and the load–displacement (P–δ) plots were captured on an interfaced computer output device and results saved in a spreadsheet.

2.7. Composite TC specimen tensile tests

The tensile testing rig with a mounted TC specimen is illustrated in Fig. 5b. The ZWICK UTM was programmed for a ramp rate of 10 mm/min. In order to capture the whole range of the stress–strain curve, failure recognition was set at 100% drop from the maximum load. Ultimate failure was by fibre rupture.

The cracking patterns on the tested samples were quantified. Crack spacings were obtained from direct linear measurements, whereas crack widths were measured with the aid of an optical microscope to a resolution of 1 μm. For each specimen, crack widths were measured at five locations that were chosen at

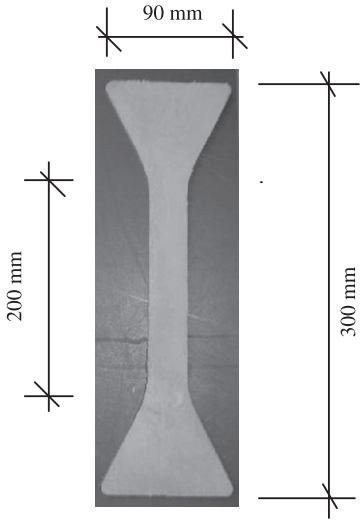

Fig. 4. Composite TC specimen.

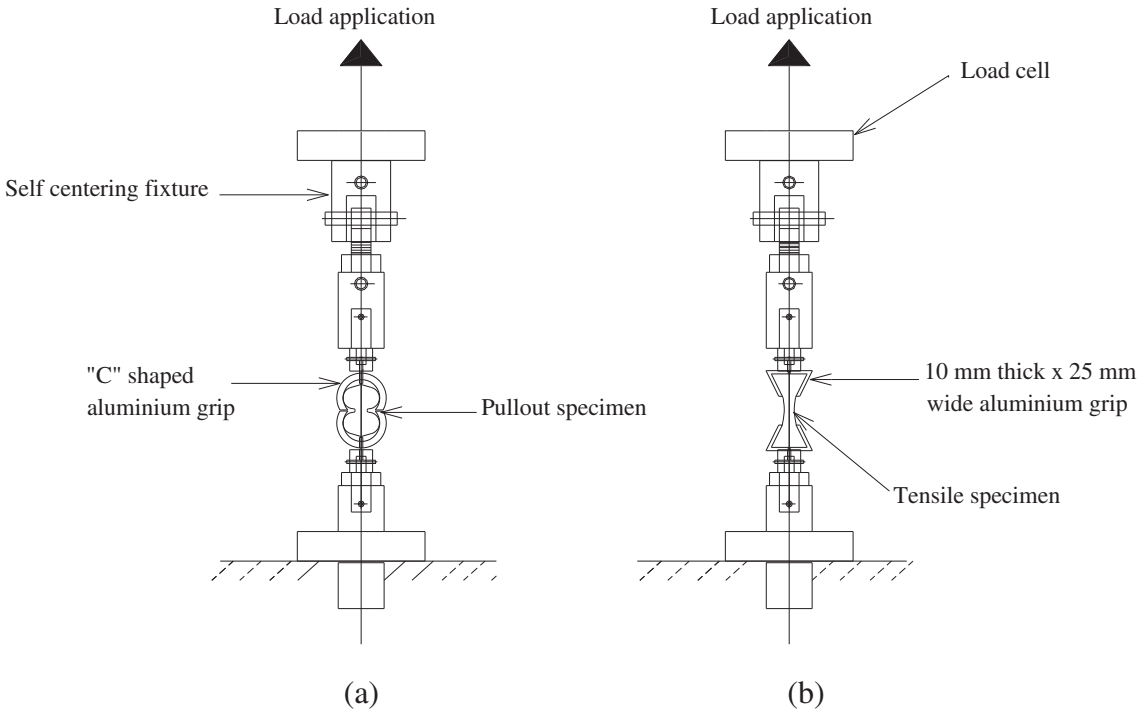

Fig. 5. Schematic of (a) fibre pull-out and (b) composite tensile test rig.

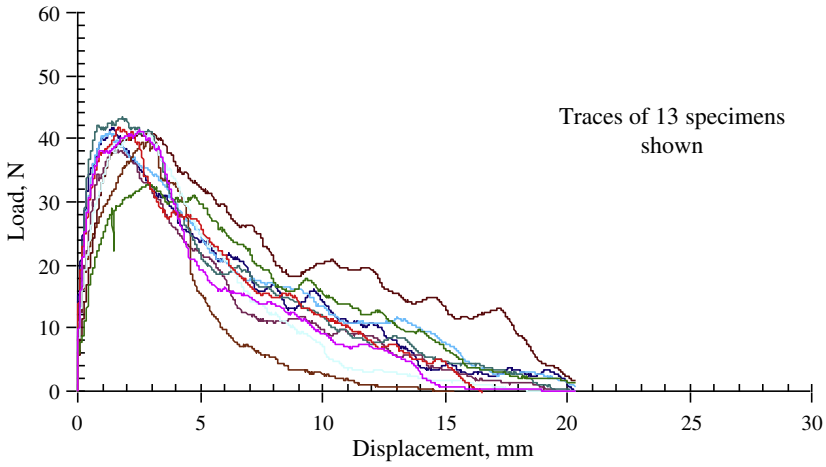

Fig. 6. Typical load–displacement traces for fibre pull-out tests.

random over the gauge sections of representative samples. The results of the number of cracks and average crack spacings are shown in Table 5.

3. Results

3.1. Constituent materials properties

The mechanical properties of fibres under different exposures were characterised by the average peak load, modulus of elasticity (E_f), and average failure strain. The matrix was characterised by the density and the average cube strength. The variation of mechanical behaviour with exposure is shown in Table 1.

Table 1 illustrates that the modulus of elasticity of the fibres was significantly affected by subjecting the fibres to 100 hot/cold cycles at temperatures varying between 23 °C and 50 °C. Table 1 also shows a significant reduction in the modulus of elasticity due to carbonation exposure.

3.2. Fibre pull-out tests

The load–deflection traces exhibited post-peak 'ductility' as shown by typical results in Fig. 6. The average values of peak load (P_{max}) were computed from the series of curves, and the average bond strength (τ) was determined from the following relationship:

$$\tau = \frac{P_{max}}{2\pi r l_e} \quad (1)$$

where r and l_e are the fibre radius and embedded length, respectively.

Table 2
Results of fibre pull-out tests (average values).

Sample	Peak load, $N \pm 2\sigma$ (σ = standard deviation) (kN)	Bond strength, τ_{max} (MPa)	Slope of load/displacement curve				Area under the curve ($J \times 10^{-3}$)
			Initial pre-peak (N/mm)	2nd pre-peak (N/mm)	Initial post-peak (N/mm)	2nd post-peak (N/mm)	
5 months control	18.72 ± 2.72	0.44	17.63	9.35	−1.55	−0.32	131.4 ± 19.1
8 months control	35.92 ± 6.46	0.84	33.91	17.46	−2.48	−0.99	271.6 ± 48.8
12 months control	35.86 ± 4.64	0.84	32.11	17.93	−3.37	−0.57	252.5 ± 13.7
Hot/cold (5 months)	18.56 ± 3.20	0.43	18.56	18.76	−2.80	−0.30	120.0 ± 20.7
Wet/dry (8 months)	34.22 ± 4.60	0.78	30.60	17.12	−2.75	−0.61	252.7 ± 34.0
Carbonated (12 months)	42.48 ± 7.98	0.99	31.78	14.16	−3.53	−0.98	384.6 ± 72.3

Table 3
Percentage change in behaviour of fibre pull-out specimens after weathering, compared to control specimens.

Sample	% Change in peak load	% Change in bond strength	% Change in slope of load/displacement curve				% Change in area under the curve
			Initial pre-peak	2nd pre-peak	Initial post-peak	2nd post-peak	
Hot/cold (5 months)	−0.85	−0.85	+5.28	+100.64	+80.65	−6.25	−8.7
Wet/dry (8 months)	−4.73	−4.73	−9.76	−1.95	+10.89	−38.00	−6.9
Carbonated (12 months)	+18.46	+18.46	−1.03	−21.03	+4.75	+71.92	+52.3

The load–displacement curves are characterised by changes in pre-peak and post-peak slopes which reflect different mechanisms and states of stress at the fibre/matrix interface. Prior to fibre debonding, elastic shear stresses exist at the interface [6] whereas microcracking of the fibre/matrix interface (during fibre debonding), induces frictional stresses. As loading progresses, the matrix undergoes damage in addition to microcracking causing the entire fibre length to debond and progressively pull-out of the matrix. With increased loading, the matrix at the interfacial zone undergoes further damage until finally no significant resistance to fibre pull-out is experienced as characterised by an asymptotic final slope.

Results of fibre pull-out tests are shown in Tables 2 and 3.

The percentage changes in peak loads and bond strengths as well as the changes of the slopes of the load/displacement curves were computed and are shown in Table 3.

3.3. Composite tensile tests

The load–displacement curves of composite specimens were characterised by an initial linear portion. This state progressed until development of microcracks, marked by a reduction in the slope of the curves. As loading progressed, there was further reduction in the slope, and perturbations of the stress–strain curves were observed. This occurred at loads in the vicinity of 1000 N (stresses between 3 MPa and 5 MPa) as shown in Fig. 7. A key feature of the stress–strain (σ–ε) curves was characteristic strain hardening and multiple cracking (propagation of several cracks), which led to the achievement of strains in excess of 20% at failure by fibre rupture. Table 3 shows the key parameters in tensile stress–strain behaviour, which were computed from the stress–strain curves of the specimens.

The stress–strain behaviour of control specimens and typical behaviour of carbonated samples are shown in Fig. 8. It is clear from the figure that carbonated samples have a higher failure stress than the controls at the same age but the toughness is significantly reduced.

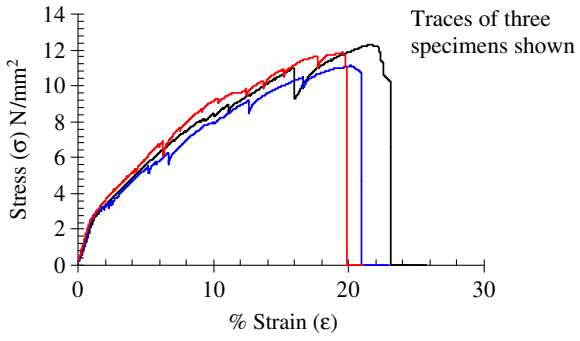

Fig. 7. Typical tensile stress–strain relationship of composites weathered by wetting/drying, tested at age 14 months.

3.4. Crack quantification

See Table 5.

4. Discussion of results

4.1. Fibre pull-out behaviour

The slopes of the fibre pull-out load–displacement curves and their physical significance are: initial slope representing an intact interface; second slope representing microcracking with some fibre debonding and mobilisation of shearing stresses along the interface; a negative post-peak slope that is manifested after the entire fibre is debonded and interface is undergoing increased damage and cracking; and the final slope, which is asymptotic to the horizontal representing minimal resistance to fibre pull-out. Mobilisation of interfacial shear that takes place at the pre-peak

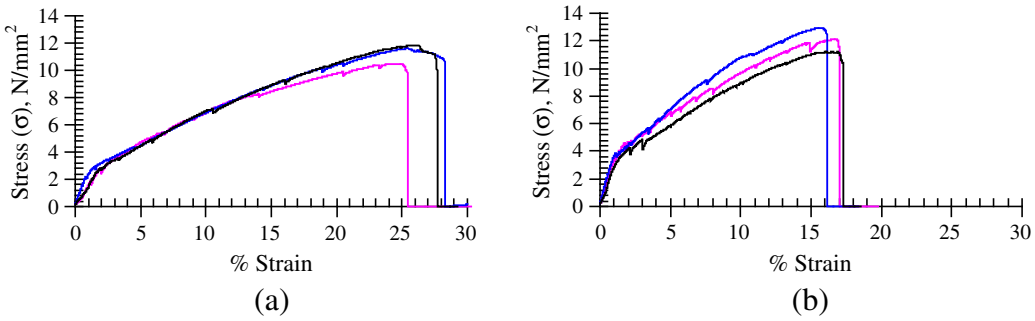

Fig. 8. Typical tensile stress–strain relationship of (a) three control samples at age 16 months and (b) three carbonated samples.

stage is associated with microcracking of the fibre/matrix interface, which influences the bond. On the other hand, the slope of the post-peak part of the load–displacement curve characterises the behaviour during fibre debonding process, and is related to fibre/matrix interface. The post-peak slopes shown in Table 1 indicate that the more brittle the fibre/matrix interface (which occurs with ageing) the steeper the slope.

Table 2 shows that there was no significant change in the peak loads after hot/cold exposure in comparison with the control samples at the same age. This behaviour was attributed to thermo-related microcracking in the matrix which counteracted the beneficial effects of elevated temperatures on fibre/matrix bonding.

Table 2 also shows a minor reduction in peak load values after wetting and drying because again, of competing mechanisms: a wetting cycle at ambient temperatures with readily available moisture would have been conducive of greater hydration and increase in fibre/matrix bonding. On the other hand, the drying cycle induced microcracks in the matrix, resulting in a reduction in the peal loads.

A small increase in pre-peak gradient is observed after hot/cold cycles as shown in Table 3, which is an indication that the fibre/matrix interfacial zone is not affected adversely by exposure to hot/cold cycles despite possible microcracking in the matrix phase.

On the other hand, there is a reduction in pre-peak gradient after wetting/drying indicating that the interface becomes less brittle. The fibre pull-out mechanism involves consumption of fracture energy for new surfaces to be formed at the microcracked zones. It is known from fracture mechanics that wet surfaces require less energy to form than dry surfaces [26]. Therefore, the reduction in post-peak gradient was possibly due to the lubricating action of moisture, which causes a reduction in frictional stresses at the fibre/matrix interface. No significant change was observed in the peak load after either cyclic hot/cold or wet/dry environments, but there was a marked increase of approximately 18% after carbonation exposure.

The results in Table 3 show that for the three weathering regimes, the initial post-peak gradient increases after weathering indicating an increase in matrix brittleness. It was observed that after the fibre pull-out test, the outer fluffy layers as well as the inner tape were damaged, which contributed to a reduction in the frictional stresses at the fibre/matrix interface. This effect was more pronounced in samples weathered in hot/cold and wet/dry environments as illustrated by a significant reduction in the final gradients in the weathered samples relative to the control samples. Conversely, a denser matrix in carbonated samples compensates for the effects of fibre damage, and therefore an increase in the final slope before failure is observed after carbonation.

The area under the load–displacement curve is a measure of energy absorption or toughness during the fibre pull-out process. As illustrated in Tables 2 and 3, carbonation exposure resulted in an increase of approximately 52% in toughness, which was attributed to matrix densification and improved fibre/matrix bonding. Conversely, hot/cold and wet/dry environments did not cause major changes in the toughness of the fibre pull-out mechanism.

The results of fibre pull-out behaviour were not sufficient to reveal: (i) how different weathering mechanisms affect the frictional shear forces at the fibril/matrix contact surfaces, and (ii) the mechanisms of fibre debonding and subsequent crack initiation and propagation.

4.2. Composite tensile behaviour

The effects of ageing and weathering on the mechanical behaviour of Textile Concrete are best understood firstly from consideration of the mechanisms governing the various slopes of fibre pull-out load–displacement curves, and secondly, from analysis of the different stages of stress–strain behaviour of the composite. These effects are related to matrix and fibre properties. The fibre/matrix interface of Textile Concrete has a complex microstructure which is influenced by interaction of fine fibrils and cement hydration products [27]. TC is in a class of composites referred to as High Performance Fibre Reinforced Cementitious Composites (HPFRCC). An important characteristic of these composites is multiple cracking (which enables large strain capacities).

The several mechanisms governing the different stages of tensile stress–strain behaviour of TC are: matrix linear tensile behaviour at low strains of less than 0.02%, matrix microcracking up to strains of approximately 2%, development of first macrocrack which traverses the sample thickness with subsequent transfer of loading from the matrix to the bridging fibres, propagation and widening of macrocracks up to peak load, crack localisation, and final failure by fibre rupture. A limitation of this research was that the test method did not provide for clear observations and evaluation of the extent of local matrix debonding at the crack planes during the tensile tests.

Densification of the microstructure was caused by cement hydration at early ages and at later ages, the effects of weathering influenced the matrix properties. These two mechanisms caused a significant increase in fibre/matrix bonding which lead to failure by fibre rupture that was manifested in all samples investigated in this research. In addition, a brittle matrix accounted for microcracking at low loading levels (up to 0.02% strain) that characterised the pre-peak stages in both fibre pull-out and composite tensile tests.

Carbonation results in deposition of calcium carbonate ($CaCO_3$) crystals in the microstructure and subsequent reduction in the average pore size [28]. The effect of deposition of $CaCO_3$ in the fibre/matrix interface is an increase in fibre/matrix mechanical interaction, which accounts for significant increase in bond strength that was observed in carbonated samples.

Table 4
Average parameters of the stress–strain curves of composite specimens.

Sample	Age (months)	End of linear region		Peak		Strain at failure (%)	Area under curve ($J/m^3 \times 10^4$)
		Stress (MPa)	Strain (%)	Stress (MPa)	Strain (%)		
Control	8	3.22	2.15	8.95	20.0	23.8	188.8
Control	12	3.25	2.00	9.91	20.3	22.3	201.5
Control	14	3.23	1.88	10.26	21.0	22.0	203.6
Control	16	2.83	1.98	11.22	25.0	30.1	260.7
Hot/cold	12	3.77	2.19	8.73	12.0	20.0	149.8
Wet/dry	14	2.99	1.36	11.43	19.0	21.0	198.8
Carbonated	16	3.95	1.79	12.33	16.0	18.0	160.3

Average values of stress and strain are stated within 15% of error.

Table 5
Crack quantification.

Sample	Age (months)	Average crack spacing (mm)	Average crack width (μm)
Control	8	5.8	141
Control	12	5.7	141
Control	14	6.7	147
Control	16	14.6	86
Hot/cold	12	5.8	77
Wet/dry	14	6.1	139
Carbonated	16	10.8	167

The extent of densification depends on ageing and exposure conditions. For example, exposure to hot/cold and wet/dry environments resulted in composites which were characterised by somewhat less post-peak ductility before final failure compared with the control of the same age (Table 4). The post-peak ductility was due to fibre softening as illustrated by a significant reduction of modulus of elasticity (E_f) after subjecting the fibres to 100 hot/cold cycles at temperatures varying between 23 °C and 50 °C (Table 1).

A wet/dry environment resulted in composites with so-called "compliant" fibre/matrix microstructures [29]. At the same time these composites exhibit post-peak ductility prior to failure (as opposed to brittle behaviour). This behaviour was accredited to favourable hydration conditions and fibre/matrix interface that sufficiently mobilised crack propagation and extension prior to final failure by fibre rupture. On the other hand, a denser matrix together with high fibre/matrix bonding that characterised carbonated samples resulted in composites with high strength (Table 4) but the microstructure was not favourable for post-peak ductility prior to failure, which was also by fibre rupture. Carbonation caused a higher gain in bond strength compared with the controls (Table 3) due to densification of the matrix at the fibre/matrix interface. This densification resulted in high composite strengths but a reduction in toughness relative to the controls (Table 4).

5. Conclusions

The following conclusions were drawn from the findings of the research on the mechanical behaviour of thin composites of a mortar matrix reinforced with several layers of woven polypropylene textiles:

1. The fibre/matrix bond strength increases with ageing under exposure to a range of accelerated weathering conditions. Textile Concrete shows minimal degradation in fibre/matrix bond under hot/cold or wet/dry exposures.
2. Carbonation resulted in an increase in bond strength of fibre/matrix specimens. The increase was attributed to deposition of calcium carbonate ($CaCO_3$) crystals in the microstructure and subsequent reduction in the average pore size of the microstructure.
3. Among the environmental regimes investigated, carbonation caused the highest gain in bond strength due to densification of the matrix at the fibre/matrix interface. To present an independent perspective of the densification of the microstructure after carbonation, topographic images of specimen fracture surfaces were obtained from scanning electron microscopy. This densification resulted in high composite strengths but militated against mobilisation of the full multiple cracking capacity in carbonated composites.
4. The results of hot/cold and wet/dry environments showed improved multiple cracking characteristics relative to control cases. A higher temperatures in a hot/cold environment increased hydration as well as softening of the fibres. In addition, cyclic heating and cooling resulted in thermal expansion and contraction, which were favourable for crack mobilisation and propagation. Deposition of hydration particles on the fibre surfaces was improved by wetting, relative to the control cases. A denser fibre/matrix interfacial microstructure had an increased load transfer between the fibre and the matrix prior to final failure by fibre rupture.

References

[1] Igarashi S, Bentur A, Mindess S. The effect of processing on the bond and interfaces in steel fiber reinforced cement composites. Cem Concr Compos 1996;18:313–22.
[2] Bentur A, Akers S. The microstructure and ageing of cellulose fibre reinforced cement composites cured in a normal environment. Int J Cem Compos Lightweight Concr 1989;11(2):99–109.
[3] Rendell F, Jauberthie R, Grantham M. Deteriorated concrete: inspection and physicochemical analysis. Thomas Telford; 2002.
[4] Addis BJ, Owens G. Fulton's concrete technology. Midrand: Cement and Concrete Institute; 2001.
[5] Savastano H, Warden PG, Coutts RS. Potential of alternative fibre cements as building materials for developing areas. J Cem Concr Compos 2003;25:585–92.
[6] Bentur A, Mindess S. Fibre reinforced cementitious composites. New York: Elsevier Applied Science; 1990.
[7] Hibbert AP, Hannant DJ. Toughness of cement composites containing polypropylene films compared with other fibre cement composites. Int J Sci Tech Reinf Mater 1982:393–9.
[8] Gilbert GT. GFRC-30 years of high fiber cement composite applications worldwide. In: Dubey A, editor. Proceedings thin reinforced cement-based products and construction systems. American Concrete Institute Publication SP-224; 2004. p. 1–20.
[9] Hesselbarth D, Kaufmann J. Properties of short fiber reinforced cement paste for concrete tubes produced by centrifugal method. In: Dubey A, editor. Proceedings thin reinforced cement-based products and construction systems. American Concrete Institute Publication SP-224; 2004. p. 112–20.
[10] Mumenya SW, Tait RB, Alexander MG. Textile concrete: preliminary mechanical characterisation of a new ductile material. In: Proceedings of the 2nd international conference of the African materials research society. Johannesburg; 2003. p. 95–6.
[11] Berstrom SG, Gram HE. Durability of alkali-sensitive fibres in concrete. Int J Cem Compos Lightweight Concr 1984;6(2):75–80.
[12] Akers AS, Studinka JB. Ageing behaviour of cellulose fibre cement composites in natural weathering and accelerated tests. Int J Cem Compos Lightweight Concr 1989;11(2):93–7.

[13] Bruckner A, Ortlepp R, Curbach M. Textile reinforced concrete for strengthening in bending and shear. Mater Struct 2006;39:741–8.
[14] Lelli VDE, Lei Z, Frieder S. Use of FRP composites in civil applications. Constr Building Mater 2003;17:389–403.
[15] Richter M, Zastrau BW. On the nonlinear elastic properties of textile reinforced concrete under tensile loading including damage and cracking. Mater Sci Eng A 2006;422:278–84.
[16] Lieboldt M, Butler M, Mechtcherine V. Application of textile reinforced concrete in prefabrication. In: Gettu R, editor. Proceedings of the seventh RILEM international symposium (BEFIB 2008) on fibre reinforced concrete: design and applications. RILEM Publications, S.A.R.L.; 2008. p. 253–62.
[17] Butler M, Lieboldt M, Mechtcherine V. Application of textile-reinforced concrete (TRC) for structural strengthening and prefabrication. In: Van Zijl G, Boshoff, W, editors. Proceedings advances in cement-based materials. CRC Press; 2009. p. 127–36.
[18] Hegger J, Sherif A, Brukermann O, Konrad M. Textile reinforced concrete: investigations at different levels. In: Dubey A, editor. Proceedings thin reinforced cement-based products and construction systems. American Concrete Institute Publication SP-224; 2004. p. 33–44.
[19] Konrad M, Chudoba R, Butenweg C, Brukermann O. Textile reinforced concrete, part II: multilevel modeling concept. In: Proceedings, international conference on the applications of computer science and mathematics in architecture and civil engineering. Weimer; 2003.
[20] Kim PJ, Wu HC, Lin Z, Li VC, DeLhoneux B, Akers SAS. Micromechanics-based durability study of cellulose cement in flexure. Cem Concr Res 1999;29: 201–8.
[21] ASTM C-230-90. Standard specification for use in tests of hydraulic cement; 1990.
[22] RILEM Committee TC14. Measurement of hardened concrete carbonation depth, CPC-18; 1988.
[23] ASTM C190-85. Standard test method for tensile strength of hydraulic cement paste; 1985.
[24] Currie B, Gardiner T. Bond between polypropylene fibres and cement matrix. Int J Cem Compos Lightweight Concr 1981;11(1):3–9.
[25] Tait RB, Guddye C. Textile concrete-mechanical characterisation of a unique fibre system for cement composites. In: Proceedings, concrete for 21st century conference. Johannesburg; 2002.
[26] Bazant Z, Gettu R. Rate effects and load relaxation in static fracture of concrete. ACI Mater J 1992;89(5):456–68.
[27] Hannant DJ. Fibre cements and fibre concretes. New York: John Wiley & Sons; 1978.
[28] Naaman A, Reinhardt H. High performance fibre reinforced cement composites HPFRCC-4. Cem Concr Compos 2004;26:754–9.
[29] Naaman A, Reinhardt H. Proposed classification of HPFRC composites based on their tensile response. Mater Struct 2006;39:547–55.